Dispersion control in two-dimensional superlattice photonic crystal slab waveguides by atomic layer deposition

D. P. Gaillot, E. Graugnard, J. Blair, and C. J. Summers

Citation: Appl. Phys. Lett. **91**, 181123 (2007); doi: 10.1063/1.2793188
View online: http://dx.doi.org/10.1063/1.2793188
View Table of Contents: http://apl.aip.org/resource/1/APPLAB/v91/i18
Published by the American Institute of Physics.

Dispersion control in two-dimensional superlattice photonic crystal slab waveguides by atomic layer deposition

D. P. Gaillot, E. Graugnard,[a] J. Blair, and C. J. Summers[b]
School of Materials Science and Engineering, Georgia Institute of Technology, Atlanta, Georgia 30332-0245, USA

(Received 9 July 2007; accepted 11 September 2007; published online 2 November 2007)

The frequency and dispersion of photonic bands in two-dimensional triangular-based superlattice photonic crystal Si slab waveguides were manipulated using atomic layer deposition. The samples were conformally coated with increasing thicknesses of TiO_2 and characterized by polarized angular-dependent reflectance measurements, which revealed shifts in the photonic band frequencies of 16% as well as continuous changes in band dispersion. The ability to tune toward zero group velocity by tuning band repulsion between same-polarization bands is demonstrated. Finite-difference time-domain calculations, combined with a dielectric weighting model, were used to assess the observed band and dispersion tuning. © *2007 American Institute of Physics*.
[DOI: 10.1063/1.2793188]

Two-dimensional photonic crystal (2D PC) slabs are being actively investigated because of their ability to control the group and phase velocity of light[1] enabling submicron beam control,[2] self collimation,[3] superprism effects,[4] and negative refraction effects.[5] Electron-beam lithography is usually employed to define the periodic dielectric modulation and integrated line, point, and periodic defects.[6] Consequently, the optical properties of 2D PC slab devices are largely determined by the precision with which the lithography process can shape dielectrics into ideal geometrical elements. Atomic layer deposition (ALD) has been shown to be an attractive tool for manipulating dielectric architectures, for both hard and soft three-dimensional (3D) PCs such as synthetic opals[7] and holographically defined polymer templates.[8] More recently, this technique was applied to silicon/TiO_2 composite 2D PC slab waveguides, and the progressive coating, and resulting air hole size reduction, shown to yield precise static tuning of the photonic band structure.[9] Additionally, TiO_2 photonic crystal waveguide structures offer the potential for low-loss and thermally stable devices.[10]

Here, we present the application of conformal TiO_2 coatings by low-temperature ALD to 2D PC slab waveguides (WGs) that possess a triangular-based superlattice (SL) pattern.[11,12] The superlattice periodicity was introduced by modifying the size of the air holes between adjacent rows of the triangular pattern. The introduction of two lattice basis points A (large hole) and B (small hole) promotes zone folding from sixfold hexagonal symmetry to twofold rectangular symmetry such that bands from the guiding region are folded into the radiating region, thus causing enhanced band-to-band interaction. The dependence of the photonic band diagrams (frequency and dispersion properties) on coating thickness was measured along high-symmetry directions by the resonant-band coupling technique[13] and compared with three-dimensional finite-difference time-domain (3D-FDTD) simulations. The progressive addition of conformal dielectric material was observed to decrease the band frequency and change the dispersion of the bands. The results reveal a large (~16%) downward shift in frequency with a precision of ~0.008% per ALD cycle for several photonic bands along all investigated directions. Furthermore, this manipulation initiates unique interactions between folded dielectric bands (TM polarization) with the subsequent flattening of interacting bands. These observations indicate that conformal ALD coating provides a powerful mechanism to adjust band dispersion and potentially the ability to tune the group velocity for ultraslow light propagation. Moreover, this technique not only enables precise postfabrication control over the dielectric contrast and geometry, but also the fabrication of devices with features sizes beyond the capabilities of current processing techniques.

A triangular-based superlattice of air holes in a 300-nm-thick single crystal silicon slab was fabricated on a silicon-on-insulator substrate by electron-beam lithography and inductively coupled plasma etching. The lattice periodicity was 360 nm with hole radii of $r_A=125$ nm and $r_B=73$ nm, as verified by scanning electron microscopy (SEM). Hence, the geometrical strength[11] of the superlattice, $r_B/r_A=0.584$. Subsequently, the sample was progressively coated with 15-nm-thick layers of amorphous TiO_2 by low-temperature ALD.[7–9] Figs. 1(a)–1(e) show top-view SEM images, before and after coating with 30, 60, 90, and 135 nm of TiO_2, respectively, for the same crystallographic directions. The systematic reductions in hole radii from 125 to 52 nm for type A and from 73 to 0 nm for type B (stage I), and then 52 to 0 nm for type A (stage II), clearly confirmed the uniformity and precision of the deposition. The SEMs revealed the ultrasmooth surface achieved by low-temperature ALD of TiO_2 (<0.2 nm rms) and the cleaved cross section in Fig. 1(f) unambiguously demonstrates the unsurpassed capability of the technique for infiltrating 2D PCs.

The primary effect on the photonic band structure is determined by the reduction in the air hole radii, which directly impacts the scattering properties of each basis point and the resulting electromagnetic field distribution for a given air or dielectric mode. The effect of thicker coatings is to uniformly reduce the diameter (and depth) of the air holes, such

[a]Current address: Department of Physics, Rollins College, Winter Park, FL 32789–4499
[b]Electronic mail: chris.summers@mse.gatech.edu

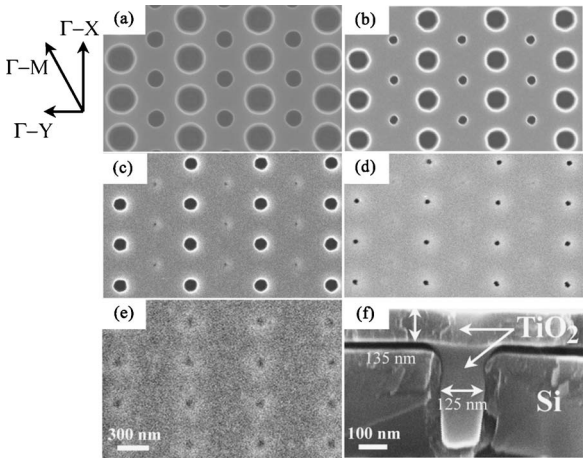

FIG. 1. Top-view SEM images of a triangular-based SL-PC Si slab WG ALD coated with TiO_2 thicknesses of (a) 0, (b) 30, (c) 60, (d) 90, and (e) 135 nm. A cleaved cross section of the coated waveguide is shown in (f) and reveals complete infiltration of the larger air holes with a solid TiO_2 plug.

as to effectively modify the dielectric contrast within the lattice. This can be quantified by calculating the dielectric weight of each basis point. By normalizing to the larger type-A holes, the smaller type-B holes can be assumed to effectively add to the structure a dielectric weight proportional to $\pi\varepsilon_{Si}(r_A^2-r_B^2)+\pi\varepsilon_{air}r_B^2$, where r_A is the radius of the larger type-A holes and r_B is the radius of the smaller type-B holes.[11,12] The effect of conformal infiltration, therefore, is to progressively change the structural configuration and the dielectric contrast of the composite slab. This can be expressed by defining an effective dielectric weight ratio K given by

$$K=\frac{\varepsilon_B}{\varepsilon_A}=\frac{\varepsilon_{Si}(r_A^2-r_B^2)+\varepsilon_{TiO_2}(r_B^2-r_B^{*2})+\varepsilon_{air}r_B^{*2}}{\varepsilon_{TiO_2}(r_A^2-r_A^{*2})+\varepsilon_{air}r_A^{*2}}, \quad (1)$$

where r_A^* and r_B^* are the reduced radii after conformal infiltration, as shown in Fig. 2(a) ($r_A^*=r_A-t$ and $r_B^*=r_B-t$, where t is the coating thickness). The dependence of K on TiO_2 layer thickness, normalized to the lattice constant a using the structural parameters of the fabricated structure, is shown in Fig. 2(b). It is observed that the initial value of K for the bare structure ($K\sim 8.18$ for $t/a=0$) decreases rapidly as the coating thickness increases from 0 to $0.05a$, and then slowly decreases and saturates to a minimum value of ~ 1.81 at which point both holes are fully infiltrated. The effective dielectric weight ε_A and ε_B of each hole also shows that K is driven by the large fractional change in ε_A as the air holes become filled. Although it appears that the presence of TiO_2 in the smaller holes adds some dielectric weight to the structure, the superlattice effect is sustained throughout the infiltration range. Also, Fig. 2(b) presents the K ratio for a Si infiltrated structure (same index as the slab). In this scenario, K decreases at a faster rate because Si has a higher index than TiO_2 and goes to unity at full infiltration indicating that the slab behaves as an optically isotropic material.

The optical properties of the composite Si/TiO_2 slab waveguide were characterized between each infiltration along the main PC superlattice directions, Γ-M, Γ-X, and Γ-Y. Data were acquired from 700 to 1700 nm using a polarized angular-resolved reflectance spectrometer to monitor the progressive modification of the radiated mode frequencies.[13,14] Also, 3D-FDTD calculations ($n_{Si}=3.45$ and $n_{TiO_2}=2.31$) were performed with a dielectric model that

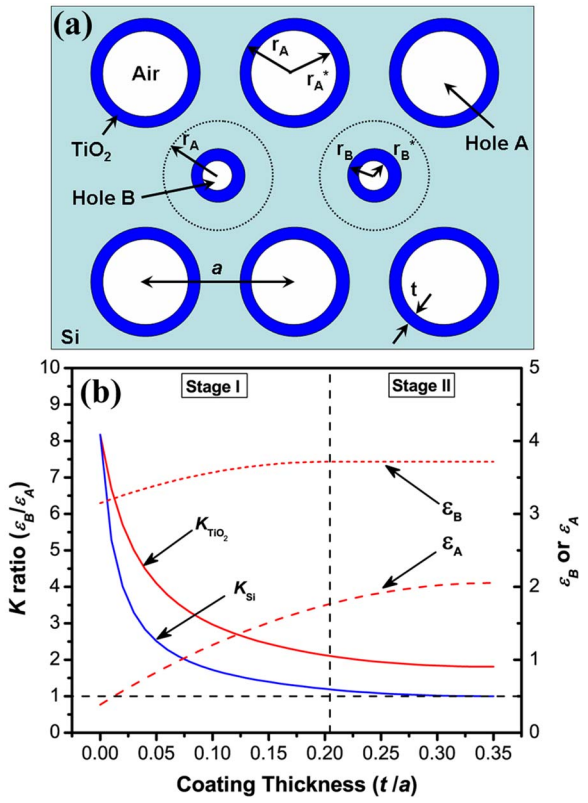

FIG. 2. (Color online) (a) 2D SL-PC geometrical model. (b) Dependence of K ratio on the thickness normalized to the lattice constant for conformal coatings of TiO_2 and Si in a 2D SL-PC with strength of 0.584. The effective dielectric weight for holes A, ε_A, and B, ε_B, is also plotted. The initial normalized radii of hole A and B are 0.35 and 0.2046, respectively. The dashed vertical line indicates when the smaller holes are fully filled.

faithfully describes the conformal deposition of TiO_2 over the entire device. The measured and simulated data for 0-, 60- and 135-nm-thick TiO_2 coatings are shown in Fig. 3 along the Γ-X direction, where the most notable effects occur. The optical measurements are in excellent agreement with the FDTD simulations for the lowest bands and in close agreement for all higher bands. The slight deviation between

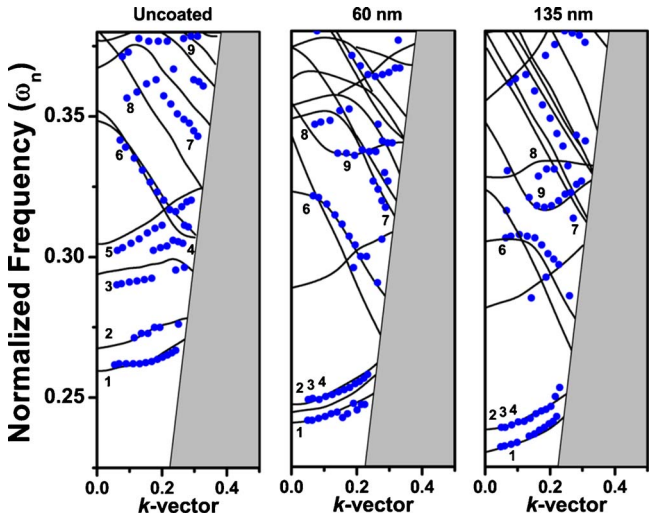

FIG. 3. (Color online) Measured (dots) and calculated (lines) photonic bands for an uncoated (left), 60 nm TiO_2 coated (center), and 135 nm coated (right) slab waveguides along the Γ-X direction. The gray region corresponds to guided modes that could not be measured.

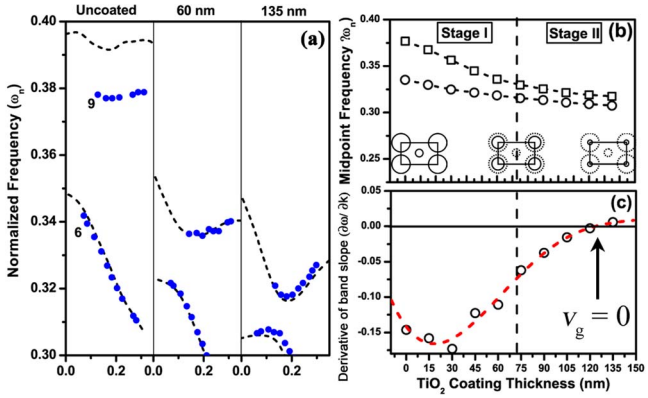

FIG. 4. (Color online) (a) Isolated plot of measured (dots) and calculated (dashed lines) TM-polarized bands 6 and 9 extracted from Fig. 3. (b) Experimentally determined frequency of bands 6 (circle) and 9 (square) from (a) along the Γ-X direction as a function of TiO_2 thickness. The schematics show the unit cell of each structure. (c) Dependence of the gradient (group velocity) on TiO_2 thickness for band 6 at a normalized wave-vector ($ka/2\pi$) value of 0.11. A zero group velocity is obtained for a 125 nm TiO_2 coating.

the simulations and data for the high-order bands is a result of the wavelength dependence of the refractive indices for both Si and TiO_2, which was not included in the FDTD calculations. Figure 3 indicates that the bands shift to lower frequencies at a rate dependent on the degree of TiO_2 infiltration. In particular, the band structure is highly modified during the early stages of infiltration (stage I) whereas slight modifications occur throughout stage II. These effects support the predictions of Fig. 2 where the effective dielectric weight ratio rapidly decreases with increasing thickness until the smaller holes are filled (stage I) and then slowly decreases until the larger holes are filled (stage II). Consequently, it is expected that the dielectric bands shift downward in frequency accordingly. Specifically, bands 1 and 2 move to lower frequency in an ordered fashion, whereas bands 3 and 4 quickly collapse into the two lower bands after 60 nm of TiO_2. Note that the measured band 5 rapidly disappeared in contrast with the computed band. Frequency shifts of $8\%-16\%$ were computed for several bands.

Although most of the bands continue to shift in frequency throughout stage II, we note that certain bands exhibit additional features. For example, a strong effect is observed between bands 6 and 9. As band 9 shifts down in frequency, it progressively interacts with band 6 such that both bands display pronounced changes in curvature with increasing infiltration, as shown in Fig. 4(a). It is well known that the gradient of the bands forming a photonic gap are strongly dependent on the energy separation between the interacting bands. Because this mechanism is only relevant for bands with the same polarization, polarization-dependent measurements were performed and confirmed that bands 6 and 9 are both TM polarized. Figure 4(b) tracks the positions of bands 9 and 6 as a function of TiO_2 deposition at normalized wave-vector ($ka/2\pi$) values of ~ 0.21 and ~ 0.11, respectively. Band 9 exhibits a rapid decrease in frequency from $\omega_n = 0.377$ to 0.317 for coatings up to 135 nm, whereas for the same conditions band 6 shifts down at a slower but constant rate from $\omega_n = 0.335$ to 0.307. Figure 4(c) plots the gradient of band 6 with increasing TiO_2 thickness at $ka/2\pi \sim 0.11$. Essentially, these data quantify the change in curvature for band 6 as the interaction with band 9 increases. Between 0 and ~ 30 nm, the gradient of band 6 decreases. However, as the structure approaches stage II, a positive monotonic behavior was observed due to the repulsion between bands. A flat band condition resulting in zero group velocity was achieved for a thickness of ~ 125 nm at which point the structure was completely infiltrated. In our previous work on a conventional triangular lattice PC, a similar condition was obtained, but the gradient exhibited a negative monotonic behavior with increasing TiO_2 thickness. The difference in gradient sign may be attributed to differences from one band to another or possibly to the folding of this particular band due to the effect of the reduced symmetry from six- to twofold along the same crystal direction. Finally, computations of the photonic band structure for Si infiltrated Si waveguide slabs for the same range of K values show no perturbation effect, indicating that composite waveguides introduce unique phenomena, which are not reproducible with a single material.

In summary, we have investigated the change in photonic band structure resulting from conformally coating a 2D triangular-based SL-PC Si slab WG with TiO_2. The dispersion properties of the folded bands were adjusted by engineering the dielectric architecture and morphology of the SL slab. The robustness and versatility of the ALD technique enable precise control over the frequency, phase and group velocities of the structure. A tuning range of 8%–16% with a precision of $\sim 0.008\%$ per ALD cycle and the initiation of optical modes with reduced/zero group velocity were demonstrated. Thus, ALD modification is a powerful approach not only to enable the formation and tuning of optical effects desirable for the achievement of electrooptical devices (light collection, sensing, amplification, processing, or routing), but also to fabricate patterns with ultrasmall geometrical elements. Although relatively unexplored, this nonconventional class of composite/multilayered architectures may unravel a wealth of unique devices with robust and enhanced optical properties.

The authors thank T. Yamashita and C. W. Neff for stimulating discussions and support from the U.S. Army Research Office under MURI Contract No. DAAD19-01-1-0603.

[1] H. Gersen, T. J. Karle, R. J. P. Engelen, W. Bogaerts, J. P. Korterik, N. F. v. Hulst, T. F. Krauss, and L. Kuipers, Phys. Rev. Lett. **94**, 073903 (2005).
[2] S. J. McNab, N. Moll, and Y. A. Vlasov, Opt. Express **11**, 22 (2003).
[3] H. Kosaka, T. Kawashima, A. Tomita, M. Notomi, T. Tamamura, T. Sato, and S. Kawakami, Appl. Phys. Lett. **74**, 1370 (1999).
[4] H. Kosaka, T. Kawashima, A. Tomita, M. Notomi, T. Tamamura, T. Sato, and S. Kawakami, Phys. Rev. B **58**, 10096(R) (1998).
[5] E. Schonbrun, T. Yamashita, W. Park, and C. J. Summers, Phys. Rev. B **73**, 195117 (2006).
[6] Z. Zhang and M. Qiu, Opt. Express **13**, 7 (2005).
[7] J. S. King, E. Graugnard, and C. J. Summers, Adv. Mater. (Weinheim, Ger.) **17**, 1010 (2005).
[8] J. S. King, E. Graugnard, O. M. Roche, D. N. Sharp, J. Scrimgeour, R. G. Denning, A. J. Turberfield, and C. J. Summers, Adv. Mater. (Weinheim, Ger.) **18**, 1561 (2006).
[9] E. Graugnard, D. P. Gaillot, S. M. Dunham, C. W. Neff, T. Yamashita, and C. J. Summers, Appl. Phys. Lett. **89**, 181108 (2006).
[10] X. Wang, M. Fujimaki, and K. Awazu, Opt. Express **13**, 1486 (2005).
[11] W. Park and C. J. Summers, Appl. Phys. Lett. **84**, 2013 (2004).
[12] C. W. Neff and C. J. Summers, Opt. Express **13**, 8 (2005).
[13] V. N. Astratov, D. Whittaker, I. Culshaw, R. Stevenson, M. S. Skolnick, T. F. Krauss, and R. D. L. Rue, Phys. Rev. B **60**, R16255 (1999).
[14] D. Coquillat, A. Ribayrol, R. M. De La Rue, M. Le Vassor d'Yerville, D. Cassagne, and J. P. Albert, Appl. Phys. B: Lasers Opt. **73**, 591 (2001).